

Supporting Information

Ultra-sensitive detection of amyloid- β using PrPC on the highly conductive AuNPs-PEDOT-PTAA composite electrode

Jieling Qin, Misuk Cho*, and Youngkwan Lee*

School of Chemical Engineering, Sungkyunkwan University, 16419 Suwon, Korea

Fax: +82-31-290-7272

Tel.: +82-31-290-7248

*Correspondence: mstop21@skku.edu (Misuk Cho) and yklee@skku.edu
(Youngkwan Lee)

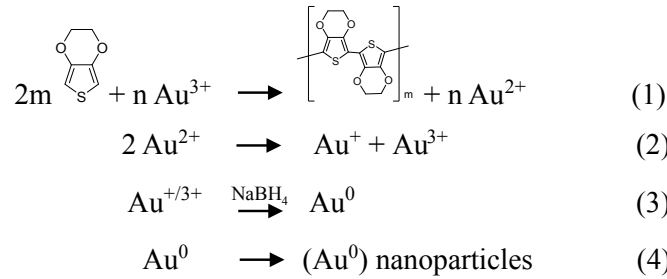
*These authors contributed equally.

Table of contents

Preparation of AuNPs	S-2
Treatment of A β solution and real sample analysis	S-3
Figure S1. Stepwise preparation of various sensors	S-4
Figure S2. Electrodeposition of PEDOT and AuNPs-PEDOT	S-4
Table S1. R_{ct} , C and area values of various electrodes	S-5
Figure S3. Nyquist plots and the goodness of fit for the proposed circuit	S-5
Figure S4. Nyquist plots of the step immobilization and sensing performance for PTAA and PEDOT-PTAA electrodes	S-6
Figure S5. CVs of the step immobilization	S-7
Figure S6. Nyquist plots of the step immobilization for 3-TAA electrodes	S-7
Figure S7. Procedure for the sampling and EIS analysis of mice	S-8
Figure S8. Selectivity of A β for monomer, oligomer and fibril	S-8
References	S-9

Preparation of AuNPs. AuNPs-EDOT/PEDOT composite was successfully synthesized by a simple redox reaction method. In a typical synthesis, the AuNPs-EDOT/PEDOT hybrid was obtained from a 50 mL aqueous solution containing 0.5 mM AuCl₃ (7.6 × 10⁻³ g) and 5 mM EDOT in an ice bath for 1 h, followed by the drop addition of 7.6 × 10⁻³ g fresh NaBH₄ with vigorous stirring. The solution was kept for 6 h at 0 °C with grape-red color. The AuNPs-EDOT/PEDOT were washed by distilled water, ethanol three times and then dried in vacuum oven.

The possible mechanism of AuNPs-EDOT/PEDOT composite was illustrated below. Specifically, during the mixing of AuCl₃ and EDOT, the Au³⁺ can be partially reduced to Au²⁺, while the EDOT itself underwent oxidative polymerization to PEDOT. ^{1,2} The unstable Au²⁺ was then disproportionate to form Au⁺ and Au³⁺. ³ Subsequently, the addition of high reductant NaBH₄ can reduce the residual Au^{+/3+} to Au⁰ followed by the formation of gold nanoparticles. The EDOT/PEDOT were incorporated on the AuNPs through the possible gold-sulfur (thiophene) interactions. ⁴ Hence, the addition of EDOT may act as weak stabilizer and reductant during the AuNPs formation simultaneously and the possible reactions showed below.



Treatment of A β solution and real sample analysis. The preparation of A β monomers, oligomers, and fibrils was performed according to previous studies.^{5,6} All animals used in the real sample analysis experiments were purchased from the Jackson Laboratory (Bar Harbor, ME, USA), and raised in the Department of Pharmacy at the Sungkyunkwan University. The experimental samples were prepared as in our previous work.⁷ Briefly, the Hemizygous 5xFAD Alzheimer's disease (AD, APPS^{wF1L}on/ PSEN1*^{M146L}*^{L286V}) and wild type (WT) mice were received as the C57BL/6J model. All the mice were free access to food and drink and raised in RT (22 \pm 2°C), humidity about 55 \pm 15% with the dark light cycle on a 12 h light and 12 h dark (lights on from 8:00 to 20:00). All the efforts were made to minimize the suffering and the number of mice we used. After that, the WT and AD mice were sacrificed at 7 month of age and their brain were collected and stored at -70 °C. The collected brain tissues were subsequently homogenized in the T-PER containing protease inhibitor cocktail and phosphatase inhibitor cocktail to obtain protein extracts followed by the incubation on ice for 30 min with the vortex at maximum speed every minute. These samples were then centrifuged at 13,000 rpm for 30 min to obtain the supernatants. Finally, the concentration of protein was calculated by using BCA assay kit, and the protein extracts were stored at -70 °C before use.

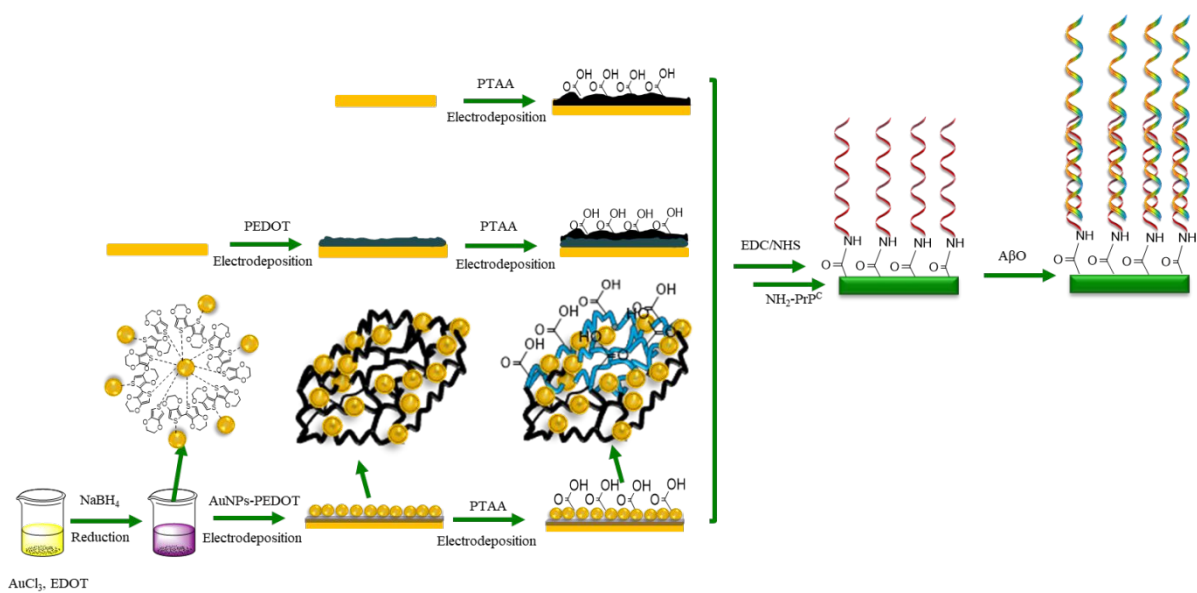


Figure S1. Stepwise preparation of PTAA/PrPC, PEDOT-PTAA/PrPC and AuNPs-PEDOT-PTAA/PrPC sensors and their A β O detection

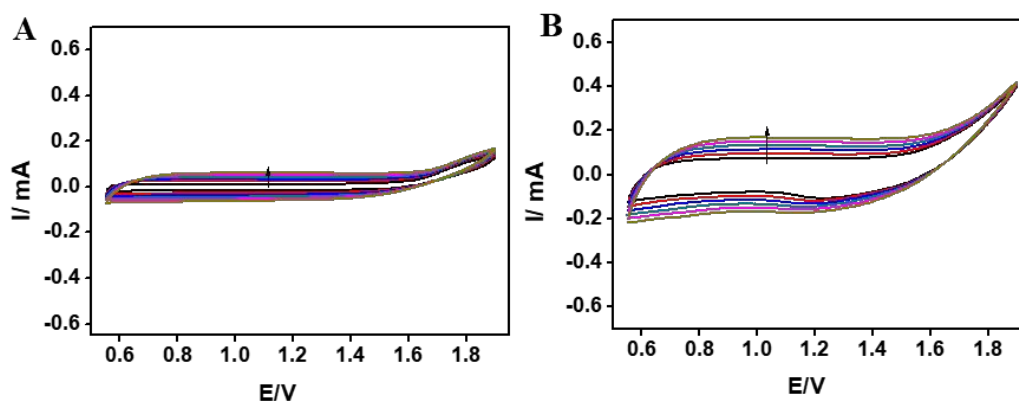


Figure S2. Electrodepositions of PEDOT (A) and AuNPs-PEDOT (B)

Table S1. The R_{et} , C and A of AuNPs-PEDOT (a), PEDOT (b), bare gold (c), AuNPs-PEDOT-PTAA (d), PEDOT-PTAA (e), and PTAA (f) electrode in 20 mM $Fe(CN)_6^{3-/4-}$ /PBS from EIS; The weight was received before/after the electrochemical polymerization of the electrodes. The specific capacitance was measured in F/g; R_{et} , C , and A represented the electron-transfer resistance, the double layer capacitance, and the surface area, respectively

Electrode	R_{et} (Ωcm^{-2})	C ($\times 10^{-7}$ F)	A ($\times 10^{-2}$ cm^2)	Weight ($\times 10^{-4}$ g)	Specific C ($\times 10^{-3}$ Fg $^{-1}$)	S_A (cm^2g^{-1})
Bare gold	65	7.2	3.6	-	-	-
PTAA	229	2.7	1.4	2	1.35	67.5
PEDOT-PTAA	184	5	2.5	6	2	100
AuNPs-PEDOT-PTAA	99	7.1	3.6	6	3.5	175

In order to find the suitable model for the fit of experiment results, four representative models were applied and tested to match the experiment data.

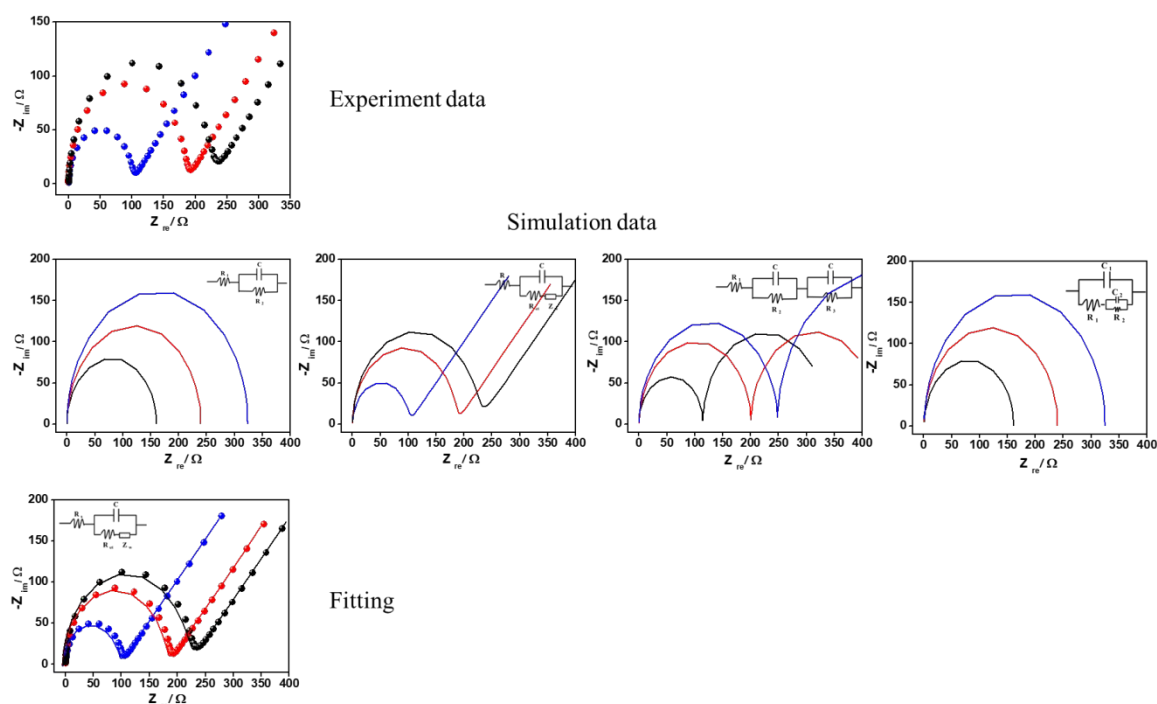


Figure S3. Nyquist plots and the goodness of fit for the proposed circuit: The equivalent circuit used to model impedance data in the form of R_s , Z_w , R_{et} , and C representing the solution resistance, the Warburg diffusion resistance, the electro-transfer resistance and the double layer capacitance, respectively

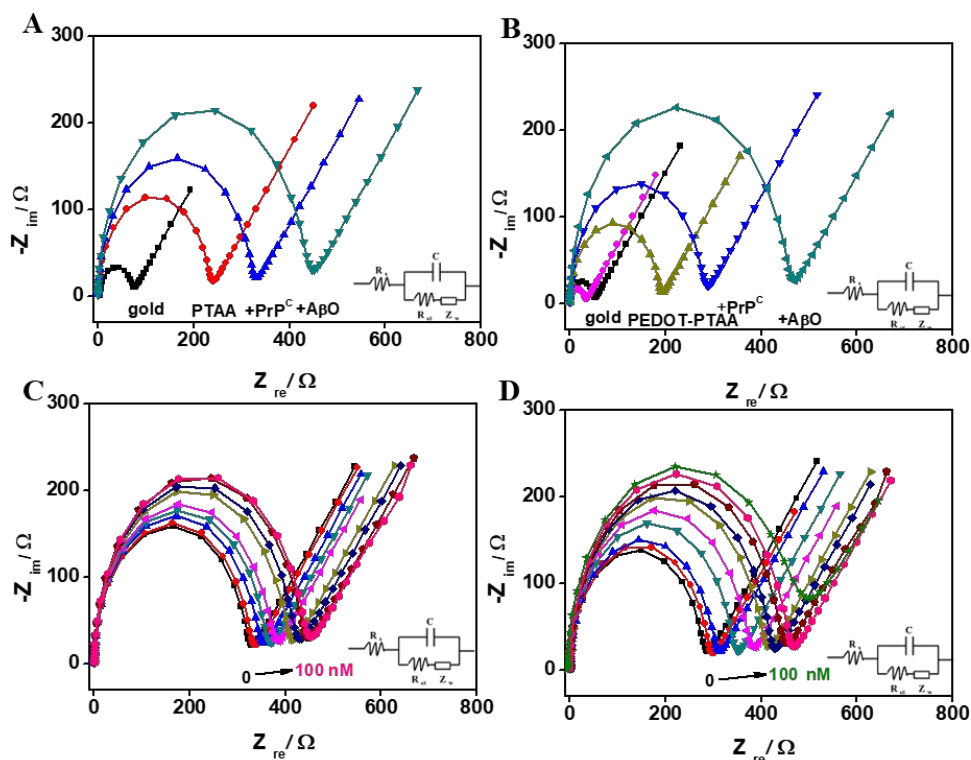


Figure S4. Nyquist plots of the step immobilization (A and B) and sensing performance (C and D) for PTAA and PEDOT-PTAA electrode in 20 mM $Fe(CN)_6^{3-/4-}$ /PBS at constant concentration of PrPC(1 mg/mL)

As shown in Figure S5 from CV, the redox current of the electrode modified with PTAA was decreased dramatically, implying the formation of a compact film on the gold surface. However, for the PEDOT-PTAA, AuNPs-PEDOT-PTAA electrode in Figure S5 B and C, the deposition of PEDOT, AuNPs-PEDOT can increase the current indicating their high surface area and excellent interface, and the followed current decrease confirmed the surface functionalization of PTAA. After the immobilization of PrPC, the redox peak currents decreased further, which indicated the peptide was successfully attached on the electrode surface. The electrode detected by AβO can act as an insulator further blocking the charge exchange of the $Fe(CN)_6^{3-/4-}$ and the gold electrode to decrease the redox peak currents.

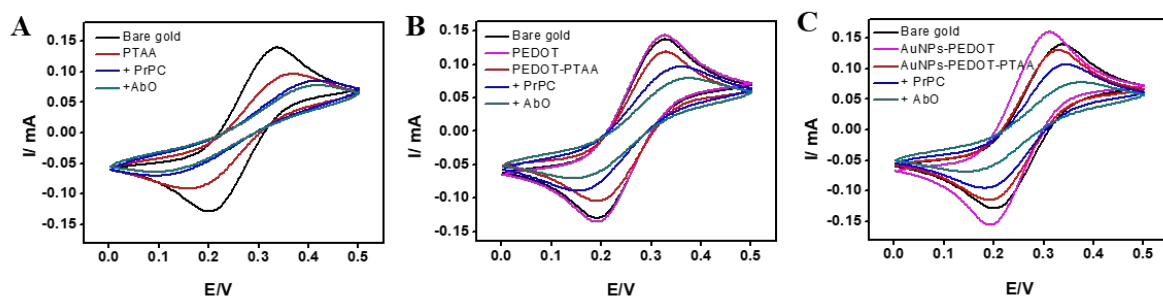
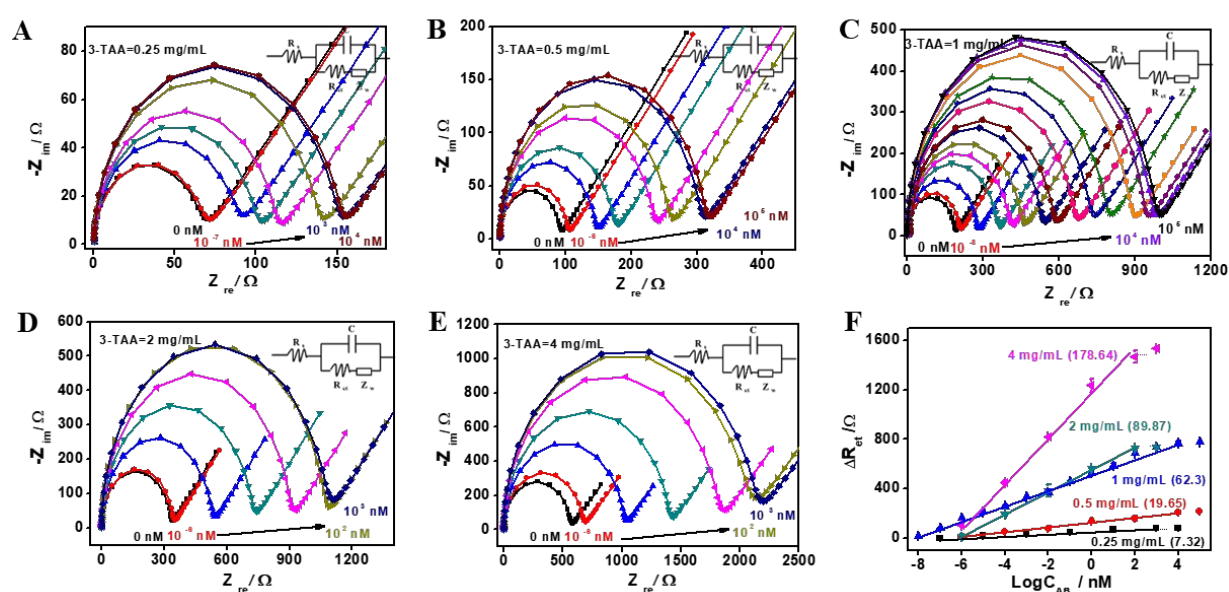


Figure S5. CVs of the step immobilization for PTAA (A); PEDOT-PTAA (B) and AuNPs-PEDOT-PTAA (C) based electrodes in PBS containing 20 mM $K_3Fe(CN)_6/K_4Fe(CN)_6$. The cultivated concentration of $A\beta O$ was 10 nM.



C_{TAA} (mg/mL)	AuNPs-PEDOT (Ω)	+ PTAA (Ω)	ΔR_{ct} (Ω)	+PrPC (Ω)	$\Delta R'_{ct}$ (Ω)	Detection range (nM)	Sensitivity ($\Omega/\log nM$)
0.25	8.173	34.62	26.45	64.59	29.97	10^{-7} - 10^3	7.32
0.5	7.924	48.01	40.09	90.65	42.64	10^{-6} - 10^4	19.65
1	6.096	98.86	92.764	186.2	87.34	10^{-8} - 10^4	62.3
2	8.095	224.8	216.71	328.5	103.7	10^{-6} - 10^2	89.87
4	7.968	412.3	404.33	559.2	146.9	10^{-6} - 10^2	178.64

Figure S6. Nyquist plots of the step immobilization for 3-TAA electrodes prepared from different concentrations of: 0.25 mg/mL (A), 0.5 mg/mL (B), 1 mg/mL (C), 2 mg/mL (D) and 4 mg/mL (E) in PBS containing 20 mM $K_3Fe(CN)_6/K_4Fe(CN)_6$. The cultivated concentration of $A\beta O$ was 10 nM. The frequency range was from 0.1 to 100 Hz with perturbation amplitude of 10 mV; Linear relationship between ΔR_{ct} value and $A\beta O$ concentration as a function of 3-TAA amount (F). The value in the bracket was sensitivity. The detailed results were summarized in a table.

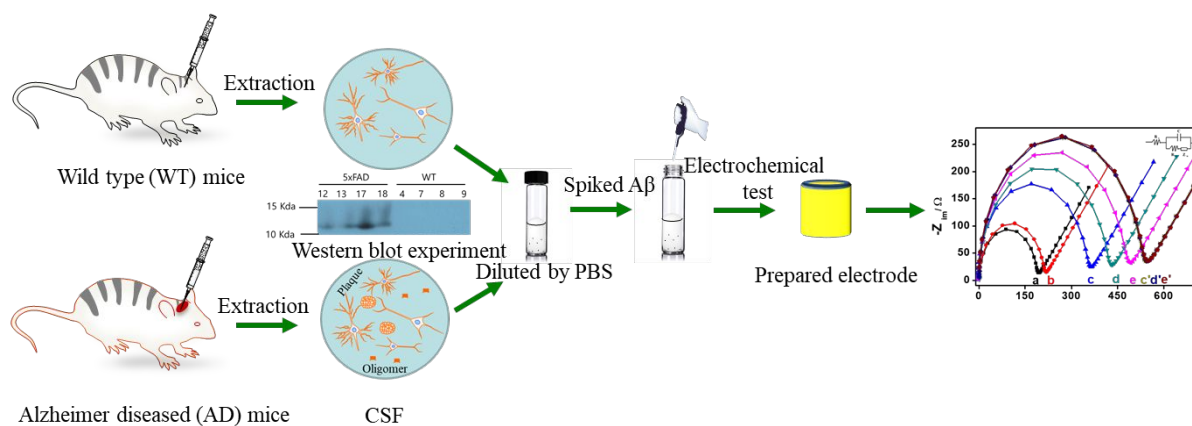


Figure S7. Procedure for the sampling and EIS analysis of WT mice and AD mice

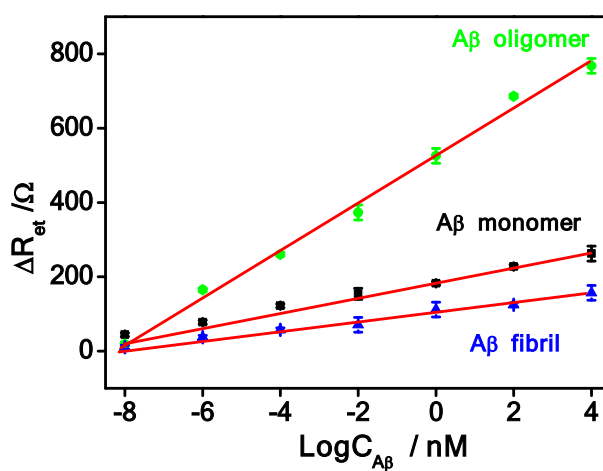


Figure S8. Selectivity of A β for monomer, oligomer and fibril

REFERENCES

- (1) Kumar, S. S.; Kumar, C. S.; Mathiyarasu, J.; Phani, K. L. Stabilized Gold Nanoparticles by Reduction Using 3,4-Ethylenedioxythiophene-polystyrenesulfonate in Aqueous Solutions: Nanocomposite Formation, Stability, and Application in Catalysis. *Langmuir* **2007**, *23*, 3401-3408.
- (2) Wang, Y.; Cai, K.; Chen, S.; Shen, S.; Yao, X. One-step interfacial synthesis and thermoelectric properties of Ag/Cu-poly(3,4-ethylenedioxythiophene) nanostructured composites. *J. Nanopart. Res.* **2014**, *16*, 2531.
- (3) Eustis, S.; Hsu, H.-Y.; El-Sayed, M. A. Gold Nanoparticle Formation from Photochemical Reduction of Au³⁺ by Continuous Excitation in Colloidal Solutions. A Proposed Molecular Mechanism. *J. Phys. Chem. B* **2005**, *109*, 4811-4815.
- (4) Selvaganesh, S. V.; Mathiyarasu, J.; Phani, K.; Yegnaraman, V. Chemical Synthesis of PEDOT–Au Nanocomposite. *Nanoscale Research Letters* **2007**, *2*, 546.
- (5) Qin, J.; Cho, M.; Lee, Y. Ferrocene-Encapsulated Zn Zeolitic Imidazole Framework (ZIF-8) for Optical and Electrochemical Sensing of Amyloid- β Oligomers and for the Early Diagnosis of Alzheimer's Disease. *ACS Appl. Mat. Interfaces* **2019**, *11*, 11743-11748.
- (6) Stine, W. B.; Dahlgren, K. N.; Krafft, G. A.; LaDu, M. J. In vitro characterization of conditions for amyloid-beta peptide oligomerization and fibrillogenesis. *J. Biol. Chem.* **2003**, *278*, 11612-11622.
- (7) Qin, J.; Jo, D. G.; Cho, M.; Lee, Y. Monitoring of early diagnosis of Alzheimer's disease using the cellular prion protein and poly(pyrrole-2-carboxylic acid) modified electrode. *Biosens. Bioelectron.* **2018**, *113*, 82-87.